



UNIVERSITY  
OF WOLLONGONG  
AUSTRALIA

University of Wollongong  
Research Online

---

Australian Institute for Innovative Materials - Papers

Australian Institute for Innovative Materials

---

2011

# Sinteractive anodic powders improve densification and electrochemical properties of BaZr<sub>0.8</sub>Y<sub>0.2</sub>O<sub>3- $\delta$</sub> electrolyte films for anode-supported solid oxide fuel cells

Lei Bi

*National Institute for Materials Science, Japan*

Emiliana Fabbri

*National Institute for Materials Science, Japan*

Ziqi Sun

*University of Wollongong, ziqi@uow.edu.au*

Enrico Traversa

*National Institute for Materials Science, Japan*

---

## Publication Details

Bi, L, Fabbri, E, Sun, Z & Traversa, E (2011), Sinteractive anodic powders improve densification and electrochemical properties of BaZr<sub>0.8</sub>Y<sub>0.2</sub>O<sub>3- $\delta$</sub>  electrolyte films for anode-supported solid oxide fuel cells, *Energy and Environmental Science*, 4(4), pp. 1352-1357.

Research Online is the open access institutional repository for the University of Wollongong. For further information contact the UOW Library: [research-pubs@uow.edu.au](mailto:research-pubs@uow.edu.au)

---

# Sinteractive anodic powders improve densification and electrochemical properties of BaZr<sub>0.8</sub>Y<sub>0.2</sub>O<sub>3-δ</sub> electrolyte films for anode-supported solid oxide fuel cells

## Abstract

The difficult sintering of BaZr<sub>0.8</sub>Y<sub>0.2</sub>O<sub>3-δ</sub> (BZY20) powders makes the fabrication of anode-supported BZY20 electrolyte films complex. Dense BZY20 membranes were successfully fabricated on anode substrates made of sinteractive NiO-BZY20 powders, prepared by a combustion method. With respect to traditional anode substrates made of powders prepared by mechanical mixing, the anode substrates made of the wet-chemically synthesized composite NiO-BZY20 powders significantly promoted the densification of BZY20 membranes: dense BZY20 films were obtained after co-pressing and co-firing at 1300 °C, a much lower temperature than those usually needed for densifying BZY20 membranes. Improved electrochemical performance was also observed: the supported BZY20 films maintained a high proton conductivity, up to  $5.4 \times 10^{-3} \text{ S cm}^{-1}$  at 700 °C. Moreover, an anode-supported fuel cell with a 30 mm thick BZY20 electrolyte film fabricated at 1400 °C on the anode made of the wetchemically synthesized NiO-BZY20 powder showed a peak power density of 172 mW cm<sup>-2</sup> at 700 °C, using La<sub>0.6</sub>Sr<sub>0.4</sub>Co<sub>0.2</sub>Fe<sub>0.8</sub>O<sub>3-δ</sub>-BaZr<sub>0.7</sub>Y<sub>0.2</sub>Pr<sub>0.1</sub>O<sub>3-δ</sub> as the cathode material, with a remarkable performance for proton-conducting solid oxide fuel cell (SOFC) applications.

## Keywords

8y0, bazr0, 2o3, electrochemical, anodic, properties, o, electrolyte, films, anode, supported, solid, oxide, fuel, cells, powders, improve, densification, sinteractive

## Disciplines

Engineering | Physical Sciences and Mathematics

## Publication Details

Bi, L, Fabbri, E, Sun, Z & Traversa, E (2011), Sinteractive anodic powders improve densification and electrochemical properties of BaZr<sub>0.8</sub>Y<sub>0.2</sub>O<sub>3-δ</sub> electrolyte films for anode-supported solid oxide fuel cells, *Energy and Environmental Science*, 4(4), pp. 1352-1357.

## Sinteractive anodic powders improve densification and electrochemical properties of $\text{BaZr}_{0.8}\text{Y}_{0.2}\text{O}_{3-\delta}$ electrolyte films for anode-supported solid oxide fuel cells†

Lei Bi, Emiliana Fabbri, Ziqi Sun and Enrico Traversa\*

Received 26th August 2010, Accepted 17th January 2011

DOI: 10.1039/c0ee00387e

The difficult sintering of  $\text{BaZr}_{0.8}\text{Y}_{0.2}\text{O}_{3-\delta}$  (BZY20) powders makes the fabrication of anode-supported BZY20 electrolyte films complex. Dense BZY20 membranes were successfully fabricated on anode substrates made of sinteractive NiO-BZY20 powders, prepared by a combustion method. With respect to traditional anode substrates made of powders prepared by mechanical mixing, the anode substrates made of the wet-chemically synthesized composite NiO-BZY20 powders significantly promoted the densification of BZY20 membranes: dense BZY20 films were obtained after co-pressing and co-firing at 1300 °C, a much lower temperature than those usually needed for densifying BZY20 membranes. Improved electrochemical performance was also observed: the supported BZY20 films maintained a high proton conductivity, up to  $5.4 \times 10^{-3} \text{ S cm}^{-1}$  at 700 °C. Moreover, an anode-supported fuel cell with a 30  $\mu\text{m}$  thick BZY20 electrolyte film fabricated at 1400 °C on the anode made of the wet-chemically synthesized NiO-BZY20 powder showed a peak power density of 172  $\text{mW cm}^{-2}$  at 700 °C, using  $\text{La}_{0.6}\text{Sr}_{0.4}\text{Co}_{0.2}\text{Fe}_{0.8}\text{O}_{3-\delta}$ - $\text{BaZr}_{0.7}\text{Y}_{0.2}\text{Pr}_{0.1}\text{O}_{3-\delta}$  as the cathode material, with a remarkable performance for proton-conducting solid oxide fuel cell (SOFC) applications.

### 1. Introduction

High temperature proton conductors are promising candidates as electrolytes for intermediate-temperature solid oxide fuel cells (IT-SOFCs) since in this temperature range they show larger ionic conductivities and smaller activation energies than conventional

oxygen-ion conducting electrolytes.<sup>1–3</sup> Until now, doped  $\text{BaCeO}_3$  and  $\text{BaZrO}_3$  dominate the research field of high temperature proton conductors.<sup>4–7</sup> Even though doped  $\text{BaCeO}_3$  materials show larger proton conductivities, they have been shown to be chemically unstable in  $\text{H}_2\text{O}$  and  $\text{CO}_2$ -containing atmospheres, resulting in electrolyte degradation and difficult fuel cell deployment.<sup>8–10</sup> In contrast, doped  $\text{BaZrO}_3$  materials are regarded to be potential candidates as electrolytes for proton-conducting SOFCs as they show an excellent chemical stability against  $\text{H}_2\text{O}$  and  $\text{CO}_2$ ,<sup>11,12</sup> as well as high bulk proton conductivity.<sup>13</sup>

Among all the doping elements, Y is the most used dopant for  $\text{BaZrO}_3$  as Y-doped  $\text{BaZrO}_3$  (BZY) shows the best proton

*International Research Center for Materials Nanoarchitectonics (MANA), National Institute for Materials Science (NIMS), 1-1 Namiki, Tsukuba, Ibaraki, 305-0044, Japan. E-mail: TRAVERSA.Enrico@nims.go.jp; Fax: +81-29-860-4706; Tel: +81-29-860-4896*

† Electronic supplementary information (ESI) available. See DOI: 10.1039/c0ee00387e

### Broader context

Energy and environmental problems are two of the major issues we are now facing for the future. With the increase in energy consumption and its negative influence on environment, new technologies are needed for electricity generation with high efficiency and low pollution. Eco-friendly solid oxide fuel cells (SOFCs) provide great potential in this aspect. However, high temperature operated SOFCs cannot meet the requirement for practical applications and to lower the working temperature is the trend in SOFC development. Among all the electrolyte materials for intermediate temperature SOFCs, proton conducting oxides provide a promising choice due to their high conductivity and low activation energy, and Y-doped  $\text{BaZrO}_3$  (BZY) is the most promising one because of its excellent stability. However, BZY is not exploited until now because it suffers from poor sinteractivity and high grain boundary resistance, which leads to low fuel cell performance and makes this material far from applications. In this study, sinteractive anodic powders were prepared by a combustion method to improve the densification and electrochemical properties of the deposited polycrystalline BZY electrolyte films, which showed a promising performance in fuel cell applications.

conductivity.<sup>2</sup> However, some distinct properties of BZY lead to a significant challenge for its practical application as electrolyte for proton-conducting SOFCs, in particular for anode-supported configuration. This is the most advantageous IT-SOFC design, since electrolyte films can greatly reduce the ohmic resistance, and thus provide improved overall cell performance.<sup>14</sup> In fact, the sinteractivity of BZY is quite poor and extremely high temperatures (up to 1700–1800 °C)<sup>9,12</sup> are needed to densify BaZrO<sub>3</sub> electrolyte membranes. The high sintering temperature not only leads to Ba evaporation that reduces conductivity, but also to the difficulty in choosing a compatible substrate material for electrode-supported fuel cells. Moreover, the difficult sintering hinders grain growth and thus a large grain boundary volume content is usually present for BZY, limiting its total conductivity, since BZY grain boundaries block proton transport.<sup>2,13</sup>

Improving the total conductivity of sintered BZY membranes still remains a great challenge. The most used strategy to overcome the BZY sintering problems is the use of sintering aids to promote its densification.<sup>15–19</sup> However, often it has been demonstrated that sintering aids reduce the BZY proton conductivity.<sup>16,17</sup> Therefore, solving the BZY densification problem without using sintering aids is desirable for fuel cell electrolyte applications. BZY20 films have been fabricated on NiO–BaCe<sub>0.7</sub>Zr<sub>0.1</sub>Y<sub>0.2</sub>O<sub>3–δ</sub> anodic substrates.<sup>20</sup> However, several reports indicated that the BaCe<sub>0.7</sub>Zr<sub>0.1</sub>Y<sub>0.2</sub>O<sub>3–δ</sub> chemical stability against CO<sub>2</sub> and H<sub>2</sub>O is insufficient for fuel cell applications.<sup>9,10,21–23</sup> A couple of studies reported the fabrication of BZY films with thickness of tens of micrometres, though the high sintering temperatures used for fabrication<sup>24</sup> and the small BZY grain size achieved<sup>25</sup> greatly limited the fuel cell performance.

It was reported that sinteractive anodes were beneficial to the fabrication of dense deposited electrolyte films at relatively lower temperatures.<sup>26,27</sup> However, the conventional BZY–NiO composite anode has been recognized to show poor sinteractivity and low shrinkage even fired at high temperatures, which is not helpful for the densification of supported BZY electrolyte films.<sup>27</sup> As a result, the preparation of dense and sintering aids free BZY electrolyte films still remains a challenge. In this study, we demonstrate that the poor sinteractivity of Y-doped BaZrO<sub>3</sub> can be overcome without the addition of sintering aids, but anode-supported BZY20 electrolyte can be densified at a temperature as low as 1300 °C when the anode is made of sinteractive NiO–BZY20 powders prepared by a combustion method. Simultaneously, improvements in BZY membrane conductivity and fuel cell performance were obtained, which is promising for SOFC applications.

## 2. Experimental procedure

NiO–BaZr<sub>0.8</sub>Y<sub>0.2</sub>O<sub>3–δ</sub> (BZY20) composite powders, in a 1 : 1 weight ratio, were synthesized by a combustion method. Stoichiometric amounts of Ba(NO<sub>3</sub>)<sub>2</sub> (99.9% purity, Wako), ZrO(NO<sub>3</sub>)<sub>2</sub>·2H<sub>2</sub>O (97% purity, Wako), Y(NO<sub>3</sub>)<sub>3</sub>·6H<sub>2</sub>O (99.8%, Aldrich) and (CH<sub>3</sub>COO)<sub>2</sub>Ni·4H<sub>2</sub>O (98% purity, Wako) were dissolved in distilled water. Citric acid was then added as a complexing agent, setting at 1.5 the molar ratio of citric acid/metal. NH<sub>4</sub>OH was added to the solution to adjust the pH value around 8. The solution was heated under stirring and finally

ignited to flame, resulting in a black ash. The ash was fired at 1100 °C for 6 h to form a fine NiO–BZY20 composite powder. The BZY20 electrolyte powder was also synthesized by the combustion method mentioned above, using Ba(NO<sub>3</sub>)<sub>2</sub>, ZrO(NO<sub>3</sub>)<sub>2</sub>·2H<sub>2</sub>O, and Y(NO<sub>3</sub>)<sub>3</sub>·6H<sub>2</sub>O as the starting materials. The BZY20 powders were fired at 1100 °C for 6 h. X-Ray diffraction (XRD, Rigaku, with Cu K $\alpha$  radiation) analysis was used to identify the phase structures of the as-prepared powders.

The BZY20 membranes were fabricated on NiO–BZY20 combustion anode substrates using a co-pressing method. The anode powder was pressed at 150 MPa into disks 13 mm in diameter and 0.8 mm thick, to obtain green substrates. BZY20 powders prepared by the combustion method and the substrates were then co-pressed at 200 MPa to form green bi-layers of anode substrate and electrolyte. BZY20 layers were fabricated also on conventional NiO–BZY20 anode substrates, in which the as-prepared BZY20 powder was mechanically mixed with commercial NiO (99.4%, Wako), which showed a single phase with particle size below 1  $\mu$ m (Fig. S1, ESI†) in a 1 : 1 weight ratio. The bi-layers were co-fired at different temperatures for 6 h in air.

The shrinkage behavior of the synthesized and the conventional NiO–BZY20 anode powders was measured from room temperature to 1400 °C using a thermal expansion analyzer (DIL 402E, NETZSCH). Scanning electron microscopy (SEM, Hitachi S-4800) was used to observe the morphology of the anode supported BZY20 electrolyte membranes. Elemental analysis of the deposited BZY20 membrane was performed using the same SEM equipped with an energy dispersive X-ray spectroscopy (EDS).

To assemble a prototype cell, a slurry consisting of La<sub>0.6</sub>Sr<sub>0.4</sub>Co<sub>0.2</sub>Fe<sub>0.8</sub>O<sub>3–δ</sub> and BaZr<sub>0.7</sub>Y<sub>0.2</sub>Pr<sub>0.1</sub>O<sub>3–δ</sub> powders mixed in a 1 : 1 weight ratio was printed on the sintered electrolyte membrane surface and then fired at 1000 °C for 3 h to form a porous cathode with an active area of 0.237 cm<sup>2</sup>. The single cell was tested at different temperatures using humidified hydrogen (~3% H<sub>2</sub>O) as the fuel and static air as the oxidant. The wet hydrogen flow was set at 50 mL min<sup>-1</sup>. The performance of the fuel cell was measured at different temperatures using a multichannel potentiostat (VMP3 Bio-Logic Co.). Electrochemical impedance spectroscopy (EIS) measurements were performed under open circuit voltage ranging the frequency from 0.1 Hz to 1 MHz, with an AC voltage amplitude of 100 mV.

## 3. Results and discussion

Fig. 1 shows the XRD pattern of the NiO–BaZr<sub>0.8</sub>Y<sub>0.2</sub>O<sub>3–δ</sub> (BZY20) anode powder prepared by a combustion method, showing mainly the presence of BZY20 and NiO. The XRD pattern is similar to that of the NiO–BZY20 anode prepared by the conventional mechanical mixing process, suggesting that the combustion method did not alter the anode phase composition. A tiny reflection peak around 32.5° for the XRD pattern of the novel NiO–BZY20 anode powder, which was ascribed to the formation of a small amount of BaY<sub>2</sub>NiO<sub>5</sub>, was also observed. It has been reported that the BaY<sub>2</sub>NiO<sub>5</sub> concentration gradually decreases with increasing the temperature but does not completely disappear, which looks like a partial decomposition of BaY<sub>2</sub>NiO<sub>5</sub>.<sup>28</sup> This partial decomposition of BaY<sub>2</sub>NiO<sub>5</sub> makes

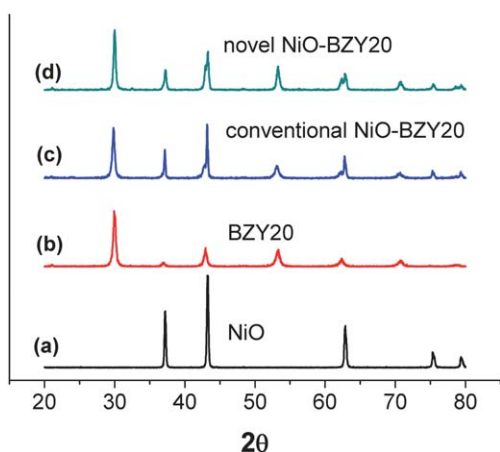


**Fig. 1** XRD patterns of (a) NiO powder, (b) BZY20 powder, (c) NiO-BZY20 composite anode powder prepared by a conventional mechanical mixing process, and (d) NiO-BZY20 composite anode powder prepared by a combustion method.

Ba, Y and Ni diffuse into the BZY grains during high temperature firing,<sup>28</sup> leading to an increase in both conductivity and sinteractivity for BZY.<sup>29</sup> Due to the formation of a small amount of  $\text{BaY}_2\text{NiO}_5$  during the powder preparation and its decomposition and diffusion into BZY20 grains, it is expected that there would be a small solubility of Ni into BZY20 perovskite structure even though there was no significant peak shift in the XRD patterns for BZY20 phase in the novel NiO-BZY20 composite anode, as compared with the XRD peaks of the conventional BZY20 powder, due to the close ionic radius between  $\text{Zr}^{4+}$  (0.72 Å) and  $\text{Ni}^{2+}$  (0.69 Å), as well as the limited solubility of Ni in BZY.<sup>16,28,29</sup>

It has been reported that a large shrinkage of the anodic substrate is beneficial to the electrolyte film densification.<sup>23,26,27</sup> During the co-sintering process for the bi-layers consisting of electrolyte and anode support, electrolyte layers shrink together with the anodic substrate. As a result, differently from the electrolyte pellet sintering, besides the grain growth of electrolyte itself, another important driving force for the densification of supported electrolyte film comes from the promotion of the anodic substrate. The more sinteractive the anodic substrate is, the stronger driving force it can provide, which would be

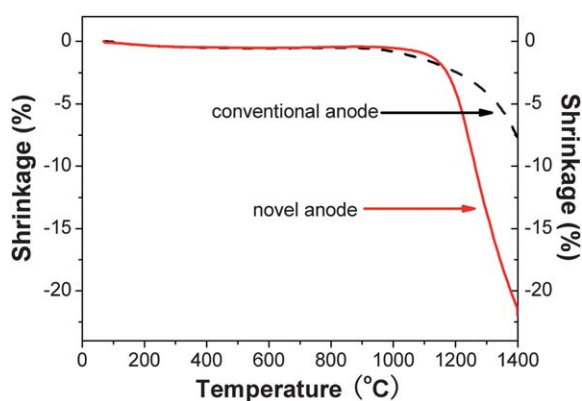


**Fig. 2** Shrinkage of the novel anode prepared by a combustion method and the conventional anode prepared by mechanical mixing.

beneficial to the densification of supported films.<sup>23,27</sup> Therefore, highly sinteractive anodic substrates are usually desirable for the fabrication of anode-supported SOFCs.<sup>20,26</sup> However, the poor sinteractivity of BZY also leads a low sinteractivity for conventional NiO-BZY anode powder.<sup>27</sup> The development of sinteractive NiO-BZY composite anode powder, which can provide a stronger driving force for the densification of supported BZY films during the sintering, could be favorable for the use in proton-conducting SOFCs with BZY electrolyte films. Fig. 2 shows the shrinkage behavior of the anode prepared by the combustion method and by the conventional mechanical mixing process, for the sake of comparison. Both the green anodes were heated from room temperature up to 1400 °C. One can observe that the shrinkage at 1400 °C of the lab-synthesized anode (21.9%) was much larger than that of the conventional anode (8.4%). The relative density of these two different anodes differed significantly after sintering at high temperatures, even though the densities of their green bodies were almost the same (Fig. S2, ESI†), suggesting that the lab-synthesized anode powder was more sinteractive than the conventional anode and their difference in shrinkage did not result from the different densities of the starting green anodes. This conclusion was further confirmed by SEM observations of the fracture surface of the anodes fired at different temperatures, showing that the lab-synthesized anodes were characterized by a less porous structure (Fig. S3, ESI†). The high sinteractivity of the lab-synthesized anode could be beneficial to promote the densification of the supported BZY films during the co-firing process, even without varying the anode composition.

As a key component of SOFCs, the electrolyte membranes should be dense to separate the fuel gas from air. Fig. 3 shows the SEM micrographs of the BZY20 membranes supported on conventional NiO-BZY20 anode substrates after sintering at 1300 and 1400 °C. The BZY20 membranes were rather porous after firing, accounting for the poor sinteractivity of BZY20, and therefore higher temperatures are needed to densify the BZY membranes. The porosity of the BZY20 films fired at 1400 °C was still too large for SOFC electrolyte applications.

Fig. 4 shows the SEM micrographs of the BZY20 membranes supported on the substrates made of the NiO-BZY20 powders

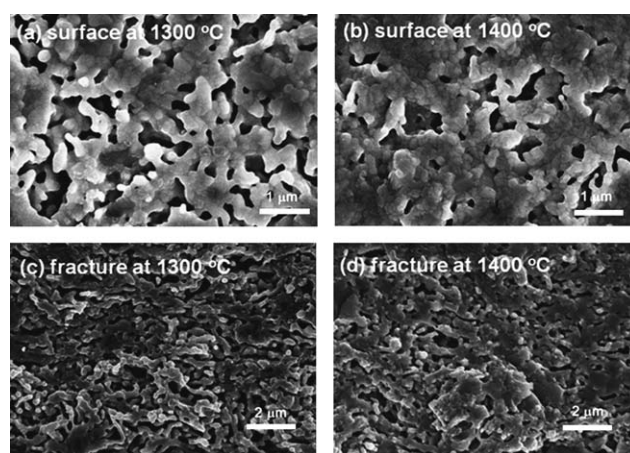


**Fig. 3** (a and b) Surface and (c and d) fracture SEM micrographs of the BZY20 membranes on the conventional anode after firing at (a and c) 1300 °C and (b and d) 1400 °C.

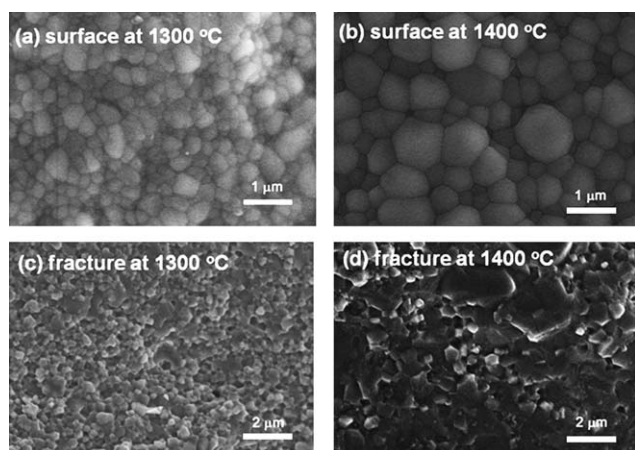


**Fig. 4** (a and b) Surface and (c and d) fracture SEM micrographs of the BZY20 membranes on the anode synthesized by the combustion method after firing at (a and c) 1300 °C and (b and d) 1400 °C.

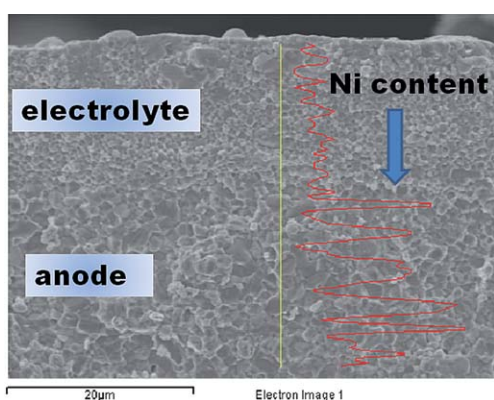


**Fig. 5** SEM-EDS analysis in line-scan mode at the interface of the BZY20 electrolyte film and the NiO-BZY20 anode.

synthesized by the combustion method after firing at 1300 and 1400 °C. Interestingly, the supported BZY20 membranes appeared dense already when sintered at a temperature as low as 1300 °C (Fig. 4a). To the best of our knowledge, 1300 °C is the lowest temperature reported to densify BZY membranes without the use of sintering aids. Given that the BZY20 membranes prepared on the conventional anode substrates were porous, this finding suggests that dense BZY20 membrane can be obtained on the novel anode substrates taking advantage of the large shrinkage that the substrate provides, facilitating the BZY electrolyte film densification. Elemental analysis was made by using SEM-EDS to investigate both the surface and fracture of the deposited BZY20 film sintered at 1400 °C (Fig. S4, ESI<sup>†</sup>). The results showed that the electrolyte contains Ba, Zr and Y, with the absence of Ni. Fig. 5 shows the Ni content in the electrolyte and anode determined by SEM-EDS line-scan mode, which indicates that the Ni content decreases from the anode to the electrolyte and the decrease at the interface is abrupt, suggesting that little Ni diffusion occurs; this result also agrees with the above elemental analysis results that showed that no Ni can be observed in the electrolyte layer. Owing to the porosity of the substrate, the larger shrinkage can be accommodated without

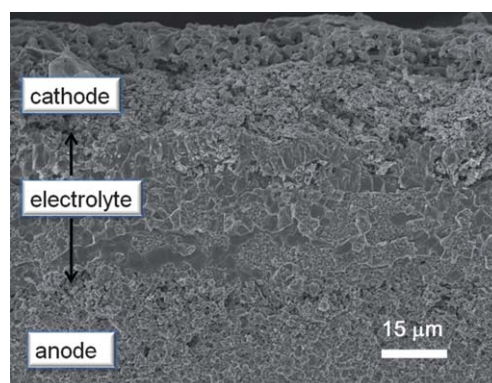


**Fig. 6** SEM cross-sectional micrograph of the single cell after testing.

film delamination. This strategy represents a facile way to overcome the sintering problems of BZY, allowing the easy fabrication of anode-supported BZY-based SOFCs without firing at extremely high temperatures and without using sintering additives, both detrimental for electrochemical performance.

However, the densification of the BZY20 films is not sufficient to guarantee a good cell performance. It has been reported that BZY films with grain size around 100 nm showed a very poor proton conductivity due to the large blocking grain boundary volume, even though the films were dense.<sup>25</sup> The grain size of the BZY20 films sintered at 1300 °C was small, about 200 nm (Fig. 4a), and therefore samples were fabricated increasing the firing temperature up to 1400 °C. At this temperature, the BZY20 grain size grew up to about 1 μm (Fig. 4b), which it is expected to be beneficial for improving the BZY20 protonic conductivity.<sup>30</sup> Therefore, fuel cell tests were performed on BZY20 samples co-fired at this temperature.

Using  $\text{La}_{0.6}\text{Sr}_{0.4}\text{Co}_{0.2}\text{Fe}_{0.8}\text{O}_{3-\delta}$ - $\text{BaZr}_{0.7}\text{Y}_{0.2}\text{Pr}_{0.1}\text{O}_{3-\delta}$  as the cathode material, anode supported single cells with BZY20 electrolyte films on anode substrates made of lab-synthesized NiO-BZY20 powders were tested. Fig. 6 presents the cross-sectional SEM micrograph of the single cell after fuel cell testing. The SEM image shows that the BZY20 electrolyte membrane was about 30 μm in thickness and quite dense, without any evident pores or cracks. The BZY20 electrolyte adhered very well with both the anode and the cathode layers, without any cracking or delamination after testing.

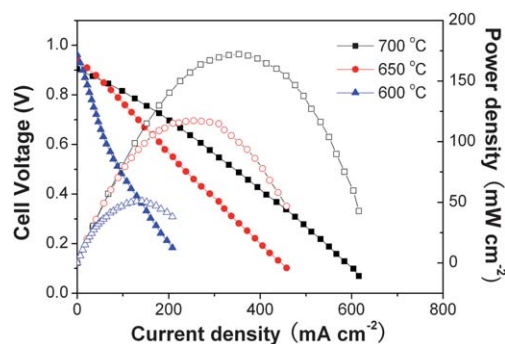


**Fig. 7** Electrochemical performance ( $I$ - $V$  and power density curves) of a prototype cell made of a BZY20 electrolyte film supported on the lab-synthesized anode, measured at 600, 650, and 700 °C.

**Table 1** Performance of fuel cells with Y-doped BaZrO<sub>3</sub> electrolyte films in literature reports and the present study

Year (reference)	BZY electrolyte thickness/ $\mu\text{m}$	Electrode substrate	Cathode material	Sintering temperature/ $^{\circ}\text{C}$	Peak power density/ $\text{mW cm}^{-2}$
2009 (21)	30	NiO–BZY	Ba <sub>0.5</sub> Sr <sub>0.5</sub> Co <sub>0.8</sub> Fe <sub>0.2</sub> O <sub>3–<math>\delta</math></sub>	1450	45 (at 700 $^{\circ}\text{C}$ )
2009 (24)	10	LSM–BZYZn <sup>a</sup>	LSM	1500	26 (at 800 $^{\circ}\text{C}$ )
2010 (20)	20	NiO–BCZY <sup>b</sup>	Sm <sub>0.5</sub> Sr <sub>0.5</sub> CoO <sub>3–<math>\delta</math></sub>	1400	170 (at 700 $^{\circ}\text{C}$ )
Present study	30	NiO–BZY	La <sub>0.6</sub> Sr <sub>0.4</sub> Co <sub>0.2</sub> Fe <sub>0.8</sub> O <sub>3–<math>\delta</math></sub>	1400	172 (at 700 $^{\circ}\text{C}$ )

<sup>a</sup> LSM: (La<sub>0.8</sub>Sr<sub>0.2</sub>)<sub>0.98</sub>MnO<sub>3– $\delta$</sub> ; BZYZn: Zn-doped BZY. <sup>b</sup> BCZY: BaCe<sub>0.7</sub>Zr<sub>0.1</sub>Y<sub>0.2</sub>O<sub>3– $\delta$</sub> .

Fig. 7 shows the  $I$ – $V$  and power density curves for the cell at different temperatures. With humidified hydrogen ( $\sim 3\%$  H<sub>2</sub>O) as the fuel and static air as the oxidant, peak power densities of 51, 117 and 172  $\text{mW cm}^{-2}$  were obtained at 600, 650 and 700  $^{\circ}\text{C}$ , respectively. The output of the cell was at least one order of magnitude larger than that of BZY electrolyte-supported cells, which was only about several  $\text{mW cm}^{-2}$  at high temperatures,<sup>5,10,24,31</sup> as the electrolyte film can greatly reduce its ohmic resistance. The performance improvement using BZY electrolyte films has been already reported in previous studies concerning electrode-supported cells fabricated using ceramic processing techniques,<sup>21,24</sup> although the present cell showed a significant improvement in the fuel cell performance, as summarized in Table 1. The cell performance in the present work is much larger and the sintering temperature used is the lowest. The obtained power output was similar to the values obtained for the BZY20 film cell fabricated on the NiO–BaCe<sub>0.7</sub>Zr<sub>0.1</sub>Y<sub>0.2</sub>O<sub>3– $\delta$</sub>  anodic substrate, but the insufficient chemical stability of BaCe<sub>0.7</sub>Zr<sub>0.1</sub>Y<sub>0.2</sub>O<sub>3– $\delta$</sub>  powder in the anode might hinder practical fuel cell applications.<sup>9,10</sup>

The good cell performance in the present study can be explained as the following: first, the densification of BZY20 membranes was obtained with the promotion of the novel anode substrates without using sintering aids, which are detrimental for BZY protonic conductivity. Second, the lower sintering temperature used here was beneficial to prevent Ba evaporation and also to avoid severe reactions between the electrolyte and the supporting substrate.<sup>16,32</sup> Third, the fine anode powder prepared

by the combustion method was more homogenous and can effectively increase the triple phase boundary (TPB) length, which results in enhancing the fuel cell performance.<sup>33</sup>

It should be noted that recently an anode-supported cell based on a thinner BZY20 film (4  $\mu\text{m}$ ), fabricated using pulsed laser deposition (PLD), showed the largest power density output for BaZrO<sub>3</sub>-based fuel cells up to now (110  $\text{mW cm}^{-2}$  at 600  $^{\circ}\text{C}$ ).<sup>34</sup> This shows that reducing the BZY20 electrolyte thickness is critical to reduce the ohmic resistance and improve cell performance. However, PLD is a technique suitable for small-scale applications,<sup>35</sup> while the strategy presented in this study to prepare BZY20 film cells might be scalable for mass production.

The electrode performance, besides the conductivity and thickness of the electrolyte film, also affects the fuel cell performance, especially at low temperatures.<sup>36</sup> Thus, EIS measurements were used to investigate the cell resistances under open circuit voltage conditions. Fig. 8 shows the typical EIS plots of the cell, measured at 600  $^{\circ}\text{C}$ , 650  $^{\circ}\text{C}$  and 700  $^{\circ}\text{C}$ . The intercept with the real axis at high frequency represents the ohmic resistance of the cell, which includes the electrolyte and lead wire resistances. The low frequency intercept corresponds to the total resistance of the cell. Therefore, the difference between the high frequency and low frequency intercepts with the real axis represents the total interfacial polarization resistance ( $R_p$ ) of the cell.<sup>6</sup> The measured ohmic resistance of the cell was 1.12  $\Omega \text{ cm}^2$  at 600  $^{\circ}\text{C}$ , 0.79  $\Omega \text{ cm}^2$  at 650  $^{\circ}\text{C}$  and 0.56  $\Omega \text{ cm}^2$  at 700  $^{\circ}\text{C}$ . If we assume that the ohmic resistance of the cell mostly comes from the electrolyte, the conductivity of the BZY20 membrane was calculated to be about  $2.7 \times 10^{-3} \text{ S cm}^{-1}$  at 600  $^{\circ}\text{C}$ ,  $3.8 \times 10^{-3} \text{ S cm}^{-1}$  at 650  $^{\circ}\text{C}$  and  $5.4 \times 10^{-3} \text{ S cm}^{-1}$  at 700  $^{\circ}\text{C}$ . These conductivity values are much larger than the conductivity values reported for tape-cast BZY films (less than  $10^{-4} \text{ S cm}^{-1}$  at 700  $^{\circ}\text{C}$ )<sup>23</sup> and for the polycrystalline BZY20 films prepared by PLD (about  $2.1 \times 10^{-4}$  at 600  $^{\circ}\text{C}$ ).<sup>34</sup> The large BZY20 electrolyte membrane conductivity in this study might be due to the successful preparation of BZY20 membrane with large grain size ( $\sim 1 \mu\text{m}$ ) without the addition of any sintering aid.<sup>25,30</sup> Although there was an improvement of conductivity for BZY20 films compared with polycrystalline BZY films reported in literatures, the conductivity was lower than that of the well-sintered BZY20 thick pellet reported by Yamazaki *et al.*, which reached  $\sim 1 \times 10^{-2} \text{ S cm}^{-1}$  at 450  $^{\circ}\text{C}$ .<sup>30</sup> Besides the processing and microstructure factors (such as different preparation method, sintering temperature, grain size) influenced the conductivity,<sup>3,25,29</sup> another factor which resulted in the difference in conductivity was the assumption we have made for the calculation of conductivity for BZY20 electrolyte films. In fact, the ohmic resistance obtained from EIS not only included

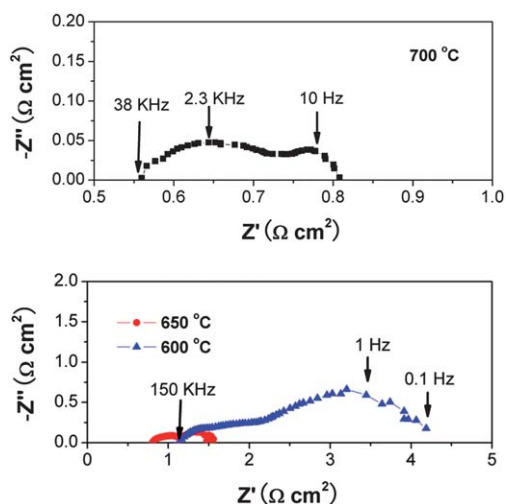


**Fig. 8** Complex-impedance plane plots of the single cell measured at 600, 650, and 700  $^{\circ}\text{C}$  in open circuit voltage conditions.

the contribution from BZY20 electrolyte but also contained the contact resistance associated with interfaces as well as the lead wires. The resistance of the electrolyte layer was part of the total ohmic resistance obtained from EIS and thus the conductivity of polycrystalline electrolyte films was usually lower than that of the thick pellet, as also reported in literatures.<sup>8,37</sup> It should be noted that the single-crystalline BZY20 film made by the PLD method showed the largest proton conductivity ever reported for BZY samples, reaching  $0.11 \text{ S cm}^{-1}$  at  $500 \text{ }^\circ\text{C}$ .<sup>13</sup> The high crystalline quality of the BZY film made it avoid the blocking effect of grain boundaries and thus led to a much enhanced conductivity, showing new potential in small-scale applications.<sup>35</sup>

The  $R_p$  of the cell were measured to be  $3.18 \text{ } \Omega \text{ cm}^2$  at  $600 \text{ }^\circ\text{C}$ ,  $0.72 \text{ } \Omega \text{ cm}^2$  at  $650 \text{ }^\circ\text{C}$  and  $0.25 \text{ } \Omega \text{ cm}^2$  at  $700 \text{ }^\circ\text{C}$ , which are values far larger than those reported in the literature for other cathodes, especially at low temperatures.<sup>38,39</sup> The ratio between the  $R_p$  and the total cell resistance increased dramatically from 31% at  $700 \text{ }^\circ\text{C}$  to 74% at  $600 \text{ }^\circ\text{C}$ , implying that the polarization resistance mainly governs the cell performance at low temperatures. The much smaller  $R_p$  value of  $0.56 \text{ } \Omega \text{ cm}^2$  at  $600 \text{ }^\circ\text{C}$ , being 23% its ratio to the total cell resistance, measured for the cell with the BZY20 film prepared by PLD,<sup>34</sup> accounts for the better fuel cell performance, despite the reduced BZY20 film conductivity. Therefore, it is reasonable to assume that a significant improvement in the fuel cell performance for the BZY cell in this study might be achieved by developing proper cathode materials and further reducing the electrolyte thickness.

#### 4. Conclusions

BZY20 membranes were successfully fabricated on anodes made of NiO–BZY20 powders prepared by a combustion method for a stable proton-conducting SOFC. The novel anode greatly promoted the BZY20 sinteractivity without any addition of sintering aids, thus maintaining the good proton conductivity of BZY20. A fuel cell based on the BZY20 membrane electrolyte showed a promising cell performance, as well as good membrane conductivity. The conductivity of the supported BZY20 membrane reached  $5.4 \times 10^{-3} \text{ S cm}^{-1}$  at  $700 \text{ }^\circ\text{C}$  and the peak power density of  $172 \text{ mW cm}^{-2}$  for cell based on the BZY20 electrolyte film was obtained at  $700 \text{ }^\circ\text{C}$ . The characteristics of both high sinteractivity and high conductivity as well as desirable cell performance for the BZY membrane in our study imply its potential applications in proton-conducting SOFCs, hydrogen sensors and hydrogen permeation membranes.

#### Acknowledgements

This work was supported in part by the World Premier International Research Center Initiative of MEXT, Japan. The authors thank Dr Hidehiko Tanaka for his invaluable technical assistance.

#### References

- 1 T. Norby, *Solid State Ionics*, 1999, **125**, 1.
- 2 K. D. Kreuer, *Annu. Rev. Mater. Res.*, 2003, **33**, 333.

- 3 E. Fabbri, D. Pergolesi and E. Traversa, *Chem. Soc. Rev.*, 2010, **39**, 4355.
- 4 N. Maffei, L. Pelletier, J. P. Charland and A. McFarlan, *Fuel Cells*, 2007, **7**, 323.
- 5 E. Fabbri, D. Pergolesi, A. D'Epifanio, E. Di Bartolomeo, G. Balestrino, S. Licoccia and E. Traversa, *Energy Environ. Sci.*, 2008, **1**, 355.
- 6 Y. Yamazaki, P. Babilo and S. M. Haile, *Chem. Mater.*, 2008, **20**, 6352.
- 7 E. Fabbri, A. D'Epifanio, S. Sanna, E. Di Bartolomeo, G. Balestrino, S. Licoccia and E. Traversa, *Energy Environ. Sci.*, 2010, **3**, 618.
- 8 C. D. Zuo, S. W. Zha, M. L. Liu, M. Hatano and M. Uchiyama, *Adv. Mater.*, 2006, **18**, 3318.
- 9 Z. M. Zhong, *Solid State Ionics*, 2007, **178**, 213.
- 10 E. Fabbri, A. D'Epifanio, E. Di Bartolomeo, S. Licoccia and E. Traversa, *Solid State Ionics*, 2008, **179**, 558.
- 11 H. G. Bohn and T. J. Schober, *J. Am. Ceram. Soc.*, 2000, **83**, 768.
- 12 K. Katahira, Y. Kohchi, T. Shimura and H. Iwahara, *Solid State Ionics*, 2000, **138**, 91.
- 13 D. Pergolesi, E. Fabbri, A. D'Epifanio, E. Di Bartolomeo, A. Tebano, S. Sanna, S. Licoccia, G. Balestrino and E. Traversa, *Nat. Mater.*, 2010, **9**, 846.
- 14 L. C. De Jonghe, C. P. Jacobson and S. J. Visco, *Annu. Rev. Mater. Res.*, 2003, **33**, 169.
- 15 S. W. Tao and J. T. S. Irvine, *Adv. Mater.*, 2006, **18**, 1581.
- 16 P. Babilo and S. M. Haile, *J. Am. Ceram. Soc.*, 2005, **88**, 2362.
- 17 N. Ito, H. Matsumoto, Y. Kawasaki, S. Okada and T. Ishihara, *Solid State Ionics*, 2008, **179**, 324.
- 18 Z. Sun, E. Fabbri, L. Bi and E. Traversa, *Phys. Chem. Chem. Phys.*, 2011, DOI: 10.1039/c0cp01470b.
- 19 L. Bi, E. Fabbri, Z. Sun and E. Traversa, *Energy Environ. Sci.*, 2011, **4**, 409.
- 20 W. P. Sun, L. T. Yan, Z. Shi, Z. W. Zhu and W. Liu, *J. Power Sources*, 2010, **195**, 4727.
- 21 Y. M. Guo, Y. Lin, R. Ran and Z. P. Shao, *J. Power Sources*, 2009, **193**, 400.
- 22 L. Bi, Z. T. Tao, C. Liu, W. P. Sun, H. Q. Wang and W. Liu, *J. Membr. Sci.*, 2009, **336**, 1.
- 23 L. Bi, S. M. Fang, Z. T. Tao, S. Q. Zhang, R. R. Peng and W. Liu, *J. Eur. Ceram. Soc.*, 2009, **29**, 2567.
- 24 C. Peng, J. Melnik, J. X. Li, J. L. Luo, A. R. Sanger and K. T. Chuang, *J. Power Sources*, 2009, **190**, 447.
- 25 J. M. Serra and W. A. Meulenber, *J. Am. Ceram. Soc.*, 2007, **90**, 2082.
- 26 J. M. Serra, O. Buchler, W. A. Meulenber and H. P. Buchkremer, *J. Electrochem. Soc.*, 2007, **154**, B334.
- 27 M. L. Fontaine, Y. Larring, J. B. Smith, H. Raeder, O. S. Andersen, M.-A. Einarsrud, K. Wiik and R. Bredesen, *J. Eur. Ceram. Soc.*, 2009, **29**, 931.
- 28 J. H. Tong, D. Clark, L. Bernau, M. Sanders and R. O'Hayre, *J. Mater. Chem.*, 2010, **20**, 6333.
- 29 J. H. Tong, D. Clark, M. Hoban and R. O'Hayre, *Solid State Ionics*, 2010, **181**, 496.
- 30 Y. Yamazaki, R. Hernandez-Sanchez and S. M. Haile, *Chem. Mater.*, 2009, **21**, 2755.
- 31 A. D'Epifanio, E. Fabbri, E. Di Bartolomeo, S. Licoccia and E. Traversa, *Fuel Cells*, 2008, **8**, 69.
- 32 M. Asamoto, H. Shirai, H. Yamaura and H. Yahiro, *J. Eur. Ceram. Soc.*, 2007, **27**, 4229.
- 33 M. Chen, B. K. Kim, Q. Xu and B. G. Ahn, *J. Membr. Sci.*, 2009, **334**, 138.
- 34 D. Pergolesi, E. Fabbri and E. Traversa, *Electrochem. Commun.*, 2010, **12**, 977.
- 35 E. Traversa, *Interface*, 2009, **18**(3), 49.
- 36 E. Fabbri, D. Pergolesi and E. Traversa, *Sci. Technol. Adv. Mater.*, 2010, **11**, 044301.
- 37 E. Fabbri, L. Bi, H. Tanaka, D. Pergolesi and E. Traversa, *Adv. Funct. Mater.*, 2011, **21**, 158.
- 38 W. Zhou, Z. P. Shao, R. Ran, W. Q. Jin and N. P. Xu, *Chem. Commun.*, 2008, 5791.
- 39 L. Yang, C. D. Zuo, S. Z. Wang, Z. Cheng and M. L. Liu, *Adv. Mater.*, 2008, **20**, 3280.